Universidade de São Paulo
Instituto de Astronomia, Geofísica e Ciências Atmosféricas
Departamento de Astronomia

Tajan Henrique de Amorim

Dust modelling in red supergiants using Bayesian inference

São Paulo
2020

Tajan Henrique de Amorim

Dust modelling in red supergiants using Bayesian inference

Trabalho de Conclusão de Curso apresentado ao Instituto de Astronomia, Geofísica e Ciências Atmosféricas da Universidade de São Paulo como requisito parcial para a obtenção do título de Bacharel em Astronomia.

Vertente: Pesquisa Básica

Orientador: Prof. Dr. Alex Cavaliéri Carciofi (IAG/USP)

São Paulo

2020

To the people I love.

Acknowledgements

Aos meus pais, Márcia e Valmir, por terem me proporcionado uma boa educação tanto escolar quanto pessoal, ensinando-me a sempre procurar entender o mundo com ceticismo;

Ao meu irmão, Marsal, por ter sido meu melhor amigo durante a nossa criação e por ter me proporcionado oportunidades de me conhecer melhor, além de me introduzir a diversos assuntos interessantes;

Ao meu orientador Alex Carciofi, por todo incentivo e amizade durante o desenvolvimento de diversos projetos durante a graduação. E aos colegas do grupo BEACON pelas discussões semanais, especialmente a Daiane, por toda ajuda no início deste projeto;

Aos principais amigos que fiz, com os quais pude aprender muito e em especial a Fabrícia, por estar comigo durante toda a graduação;

À FAPESP, pelo apoio financeiro, sob o projeto n^o: 2018/26380-8;

Àо CNPQ, ao IAG e à USP, pelo apoio financeiro e institucional.

"*Consistency is the playground of dull minds*"

Yuval Noah Harari

Resumo

Estrelas supergigantes vermelhas são estrelas massivas, da pós-sequência principal, que perdem grandes quantidades de massa, formando uma densa ejeção circunstelar. Como são frias, com temperaturas efetivas entre 3500 e 4500 K, grandes quantidades de grãos de poeira são formadas na matéria ejetada. A distribuição de energia espectral (SED) geralmente é a principal fonte de informação sobre a poeira circunstelar nesses objetos, carregando informações de quanta radiação ultravioleta e visível da estrela é reprocessada no domínio infravermelho (dando origem ao chamado excesso de infravermelho).

O objetivo deste projeto é modelar as características desses grãos e sua distribuição espacial na supergigante vermelha VY CMa. Esta estrela tem uma longa história observacional e, portanto, uma SED bastante completa está disponível para este estudo. A nova abordagem aqui proposta é combinar o código HDUST, que realiza a transferência radiativa, com a inferência bayesiana baseada nas técnicas de *Monte Carlo Markov Chain* (MCMC). A inferência bayesiana permitirá que os vários parâmetros envolvidos na modelagem sejam colocados em perspectiva, assim como o papel relativo de cada um na modelagem da SED e suas correlações, extraídas a partir das probabilidades posteriores fornecidas pelo método MCMC.

Modelos com distribuições de tamanho de grão foram cuidadosamente analisados usando o conceito de invariância aproximada, para investigar quais informações a SED fornece sobre paramêtros fundamentais do grão, tais como tamanho, temperatura e quantidade. Como utilizamos uma SED com amplo domínio espectral, $0.2 \lesssim \lambda \lesssim 200\,\mu$m, pudemos obter resultados muito precisos para a distribuição de tamanho de grão. Nossos resultados indicam que o envoltório de poeira em torno de VY CMa é bastante denso, com $\tau_V \approx 9.79$. Este envoltório reprocessa aproximadamente 91.9% da luz estelar para o domínio do in-

fravermelho. O raio interno da camada de poeira é de $13.03\,R_\star$, o que corresponde a uma temperatura de 1075 K. Os parâmetros mais prováveis indicam a presença de grãos com uma grande faixa de tamanhos ($0.002 \pm 0.001 < a < 158^{+23}_{-3}\,\mu$m) e com um distribuição dada por uma lei de potência com $q = 3.47^{+0.03}_{-0.01}$. O valor de q é especialmente interessante pois este é muito próximo do encontrado para o meio interestelar, o qual é enriquecido pelos grãos de estrelas supergigantes.

Abstract

Red supergiant stars are massive, post-main sequence stars that lose large quantities of mass, forming a dense circumstellar outflow. Since they are cold, with effective temperatures between 3500 and 4500 K, large quantities of dust grains are formed in the ejected matter. The spectral energy distribution (SED) is usually the main source of information about the circumstellar dust in these objects, and carry information of how much ultraviolet and visible radiation from the star is reprocessed into the infrared domain (originating the so-called infrared excess).

The goal of this project is to model the characteristics of these grains and their spatial distribution in the red supergiant VY CMa. This star has a long observational history, and therefore a quite complete SED is available for this study. A novel approach here proposed is to combine the HDUST code, that performs the radiative transfer, with a Bayesian inference based on Markov Chain Monte Carlo techniques (MCMC). The Bayesian inference will allow for the many parameters involved in the modelling to be put in a seamless perspective, the relative role of each one on shaping the SED, as well their cross-correlations, apparent from the posterior probabilities provided by the MCMC method.

Models considering grain size distributions were carefully analyzed in the framework of the approximate invariance concept, to investigate which information the SED can (or cannot) yield about fundamental grain parameters, such as size, temperature and quantity. As a SED covering a wide range of wavelengths was considered, $0.2 \lesssim \lambda \lesssim 200\,\mu$m, we were able to obtain very precise results for the grain size distribution. Our results indicate that the dust surrounding VY CMa is quite dense, with $\tau_V \approx 9.79$. This circumstellar dust reprocesses approximately 91.9% of photons to the infrared domain. The inner radius of the dust layer is $13.03\,R_\star$, which corresponds to a temperature of 1075 K. The most probable parameters indicate the presence of grains with wide range of sizes ($0.002 \pm 0.001 < a <$

158^{+23}_{-3} μm) and a distribution associated with a power-law of $q = 3.47^{+0.03}_{-0.01}$. The value of q is especially interesting because it is very close to that found for the interstellar medium, which is enriched by grains of supergiant stars.

List of Figures

List of Tables

Contents

Chapter 1

Introduction

1.1 Supergiant Stars

When a massive star (with initial mass of at least $\sim 8\,M_{\odot}$) ceases fusing hydrogen in its core, after spending $\sim 10^6$ to 10^7 years on the main sequence, it generally becomes a supergiant star, an enormous star that in the early post-main sequence phase fuses helium, producing carbon or oxygen trough the triple-α process (Levesque 2017). After this phase is over, the star starts the fusion of heavier elements, like carbon and oxygen, creating shells with different chemical compositions, described as an "onion skin" surrounding an iron core. When this occurs, the star collapses into a supernova and then evolves into a black hole or a neutron star.

Red supergiant stars (RSGs) bear this name for their low effective temperatures, around 3500 and 4500 K, which grant them M or K spectral types. RSGs are the largest stars in the universe, with a radius of 100 to 1000 times the solar radius, even though they are not the most massive ones, with masses between 8 and 40 solar masses (Levesque 2017). They are well known for their large luminosity, around 100,000 and 500,000 times the solar luminosity.

Nowadays, it is estimated that massive stars lose more than half of their mass after they leave the main sequence, and a significant fraction of it occurs during the RSG phase (Stothers and Chin 1996), when the surface gravity is at its lowest. As a result, a very dense circumstellar outflow is formed, where molecules and dust grains are produced once the gas cools down to sufficiently low temperatures. The site of molecular and dust formation is still not well known, as it depends on the gas temperature and the properties of the refractory material produced (Levesque 2017).

Some mechanisms have been proposed to explain how the strong outflow is driven. The most widely accepted one proposes a stellar wind driven by radiation pressure on dust grains. However, there are several complicating factors that suggest this explanation is incomplete. Other hypotheses indicate radial pulsation, dissipation of Alfvén waves, supra-Eddington mass loss, but the relative role of each mechanism is still very much open to debate. All these processes are discussed in the recent book of Levesque (2017).

1.2 Main goals

To study this mass ejection and subsequently the dust properties we analyze the Spectral Energy Distribution (SED) of a star. The SED, as observed from Earth, must be corrected by the interstellar reddening, in order to compensate from the modifications caused by the interstellar medium. Once this correction is done, the intrinsic SED becomes a rich source of information about the central star and its circumstellar material and may be in some cases the best information source, sometimes the only source, about the dust itself.

In this project, our goal is to understand to what extent the SED can be used to infer the properties of the circumstellar grains (composition, size distribution, etc.). The grains affect the SED basically in two ways: they absorb radiation at shorter wavelengths (ultraviolet – UV – and visible) and reemit the energy in the infrared (IR) part of the spectrum. This process is known as "reprocessing", and causes the well-known IR excess observed in RSGs and other dusty objects such as young stellar objects (YSO), asymptotic giant branch (AGB) stars, etc.

In addition, studying the dust properties, such as its size, density and composition can help shed light on the dust grain formation processes. More importantly, a detailed analysis of how the dust properties affects the SED can provide the means to measure the dust mass in the envelope that, in turn, may be used to estimate the mass loss rate of the star. It follows that dust grain studies, such as the one proposed in the project, may, in the long term, help us understand better the mass loss mechanism in RSGs.

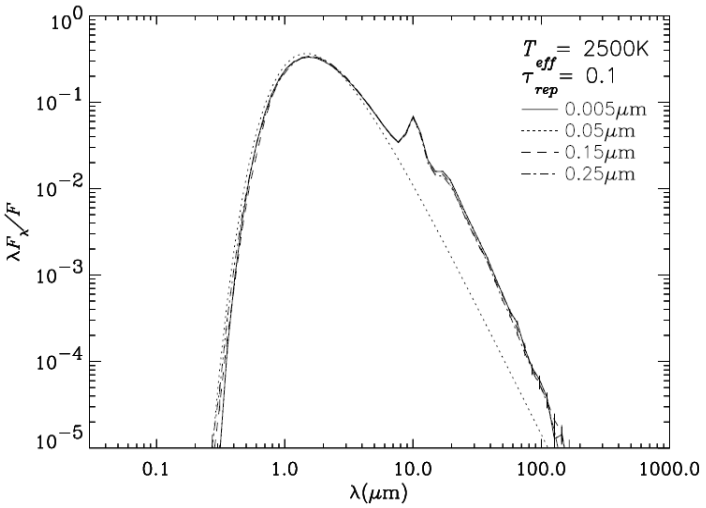

Figure 1.1: Single grain size models for optically thin envelopes (i.e. low $\tau_{\rm rep}$), with internal temperature $T_{\rm int} = 1000\,{\rm K}$, which is the temperature of the inner parts of the envelope. Shown are the results for four envelope models of cosmic silicate grains (Ossenkopf et al. 1992), with sizes $a = 0.005$, 0.05, 0.15, and 0.25 μm. Also shown is the stellar spectrum (dotted line). Reproduced from Carciofi et al. (2004).

1.3 Approximate invariance

One of the difficulties in determining the size of dust grains using only the SED is explained by the concept of approximate invariance, which derives from the fact that differently sized grains have similar optical properties at long wavelengths, leading to similar SEDs, as shown by Carciofi et al. (2004). These authors studied the effects of grain size in the SED originating from spherical envelopes and showed that under some conditions the SEDs from models with different grain sizes may be very similar. The most important condition is that different models have the same reprocessing optical depth and temperature. The reprocessing optical depth, $\tau_{\rm rep}$, is defined as

$$1 - e^{-\tau_{\rm rep}} \equiv \frac{L_{\rm rep}}{L_\star}\,, \tag{1.1}$$

where $L_\star$ is the stellar luminosity and $L_{\rm rep}$ is the fraction of the stellar luminosity that is reprocessed (i.e., absorbed and reemited) by the envelope. It follows from their work that, for a fixed grain temperature structure, the reprocessing optical depth is the only unambiguous parameter that can be extracted from the observations. Fig. 1.1, reproduced

from Carciofi et al. (2004), illustrates the concept of approximate invariance. Models that have very different grain sizes, and thus different optical properties, have a very similar SED because all models reprocess the same fraction of the stellar luminosity (approximately 10%, in this case). Another condition for approximate invariance to hold is that the optical properties of the grains have a similar shape in the spectral domain of interest. In practice, as discussed by Carciofi et al. (2004) this condition holds as long as the grain sizes considered are not widely different from each other. In this project we intend to use the concept of approximate invariance and, for the first time, following the same line of thought as used by Carciofi et al. (2004), apply it for the study of a real star.

The answer to the question of how much information on the dust grain properties (size, composition) is imprinted on the SED is very important, as the SED is in general the only source of information about the dust grains. This will be achieved by applying a robust statistical treatment that will reveal the posterior probabilities of the parameters (given the model assumptions and the data) as well their cross correlations to the supergiant star VY Canis Majoris (VY CMa).

1.4 VY CMa

The star VY Canis Majoris (VY CMa), which is classified as a red supergiant star, is one of the biggest stars in the known universe with a radius of 1420 $R_\odot$ (Wittkowski et al. 2012). Because of its gigantic radius, it has a low superficial temperature, around $T_{\rm eff} \approx 3490\,{\rm K}$, which is compensated by its size granting it a luminosity of 270,000 $L_\odot$, one of the most luminous stars in the sky (Wittkowski et al. 2012). It is believed that VY CMa is near the end of its life. Being so bright and well-studied, there is a large amount of data available, which makes it the perfect target for this study.

Current observations suggest that VY CMa loses more than $2 \times 10^{-4}\,{\rm M_\odot yr^{-1}}$ (Danchi et al. 1994), which places it as the third brightest object in the sky at 10 μm (Joint Iras Science 1994), not taking into account objects in our solar system. As said before, the mechanisms behind this mass loss are still unclear. The presence of large grains in VY CMa's surroundings was observed through polarimetry by Scicluna et al. (2015), they suggest a maximum grain size of at least $a_{\rm max} = 0.5\,\mu{\rm m}$. The material that was expelled by the star is typically organized in clumps around it, which can be observed trough

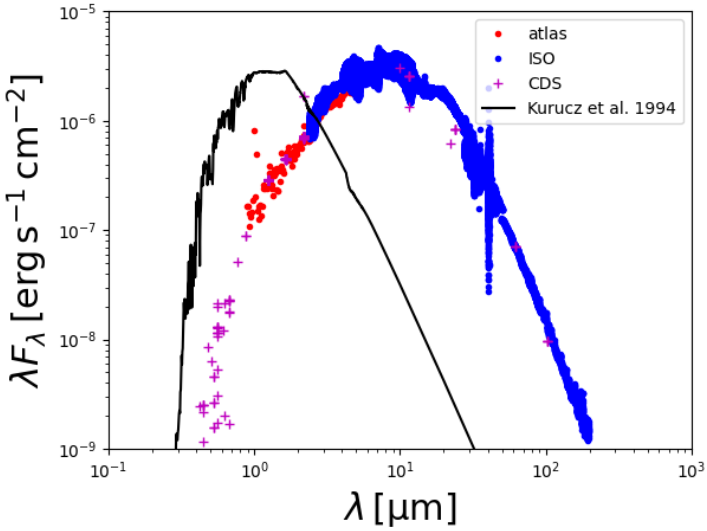

Figure 1.2: In black, a photospheric model with $T_{\rm eff} = 3500\,\mathrm{K}$ and $\log(g[\mathrm{cgs}]) = 0$ from Kurucz (1994). The points correspond to VY CMa's observed SED. The data was taken from ATLAS (Shanks et al. 2015), the Infrared Space Observatory (ISO) and the CDS portal [1].

polarimetry. In this project however, we approximate the surrounding dust as an spherical shell, because the presence of clump introduces a much more complex modelling effort.

Figure 1.2 represents the observed SED of VY CMa compared to a photospheric model (continuous line) with $T_{\rm eff} = 3500\,\mathrm{K}$ and $\log(g[\mathrm{cgs}]) = 0$ from Kurucz (1994). The reprocessing effect can be seen, in this Figure, as the SED in the IR domain lies much above the photospheric flux level, owing to dust emission. It is clear from the image that the dust visibly decreases the amount of UV light, by absorbing higher energy photons, and increasing the flux at longer wavelengths due to the grain thermal emission.

[1] ISO archive can be acessed in `http://nida.esac.esa.int/nida-cl-web/`. CDS portal, in `https://cdsportal.u-strasbg.fr/?target=VY%20CMa`.

Chapter 2

Methodology

2.1 Model description

The theoretical SEDs for VY CMa are generated by the HDUST code (Carciofi et al. 2004, Carciofi and Bjorkman 2006, Carciofi and Bjorkman 2008). HDUST is a Monte Carlo radiative transfer code that solves the coupled problem of the radiative transfer and radiative equilibrium in both gaseous and dusty media (see Figure 1.1 for examples of models calculated with HDUST). The central star was defined by the parameters contained in Table 2.1 and we adopted the stellar spectra of Kurucz (1994) to represent the stellar spectrum. The stellar parameters are held fixed in this study.

The dust envelope is considered in our models as a spherical shell, with an outer radius of $R_{\rm ext} = 200\,R_\star$ ($R_\star$ stands for stellar radius) and internal radius, $R_{\rm int}$, as a free parameter. The grain number density (n) is parameterized by,

$$n = n_0 \cdot \left(\frac{R_{\rm int}}{r}\right)^2 , \tag{2.1}$$

where n_0 is the base number density and r is the distance from the center of the star. Another important parameter of the dust envelope is $T_{\rm int}$, the dust temperature at $r = R_{\rm int}$.

2.2 Dust composition

In order to decide the dust chemical composition that better matches VY CMa, we compared different materials, whose optical constants, given by the complex refraction

Table 2.1 - Adopted stellar parameters for VY CMa (Wittkowski et al. 2012). $M_\star$ corresponds to stellar mass, $R_\star$ to stellar radius, $T_{\rm eff}$ to effective temperature, $L_\star$ to stellar luminosity, $log(g)$ to the logarithm of the surface gravity and $V_{\rm rot}$ to rotational speed.

Parameters	$M_\star[M_\odot]$	$R_\star[R_\odot]$	$T_{\rm eff}[K]$	$L_\star[L_\odot]$	$log(g)$	$V_{\rm rot}[km/s]$
Values	17	1420	3490	2.7×10^5	-0.6	40

index as a function of wavelength, are available at DOCCD [1]. In addition, some well known optical constants, used by codes such as DUSTY [2], were also considered. We selected only the materials for which the optical constants were available for the wavelength range for which data was available (0.2μm $< \lambda <$ 200 μm), leading to 14 possible materials.

Due to the presence of strong SiO masers (know for a long time, Scalise Jr and Lepine 1978), VO and TiO emission (Humphreys et al. 2019), VY CMa is considered in the literature as an oxygen-rich star, which strongly argues in favor of silicate grains being the predominant dust composition in this star. Removing the non amorphous silicate grains from the sample leads us to 6 remaining materials. Figure 2.1 shows the optical depth for each of the 6 materials, calculated with single grain sized models of $a = 0.15\,\mu$m, $R_{\rm int} = 10\,R_\star$ and $\tau_{\rm V} = 10$. It is possible to see, 2 groups of grains, the ones containing magnesium (*pyrmg80* and *mg15*) and the ones without it. We have arbitrarily decided to use the optical constants of the astronomical silicate of Ossenkopf et al. (1992), from the homogeneous group without magnesium. This choice is supported by the the minimal difference in optical depth between each silicate material without magnesium and that, as seen in Figure 2.1, grains with magnesium should produce much fainter flux in the far infrared region, which does not correspond to the observed SED (Fig. 1.2).

2.3 Grain size distribution

Almost all systems in nature are in reality distributions of values, leading to striking differences if compared to the physical models which consider discrete values. However, the distribution that best represents a phenomena is generally not easy do discover. In this project, the grain size, which is a very important and studied parameter, faces this issue, as a distribution of grain sizes is expected for the circumstellar environment. In the

[1] The Database of Optical Constants for Cosmic Dust of the laboratory Astrophysics Group of the AIU. Jena can be accessed in `https://www.astro.uni-jena.de/Laboratory/OCDB/index.html`

[2] DUSTY code , from Ivezic et al. (1999), can be accessed in `https://github.com/ivezic/dusty`.

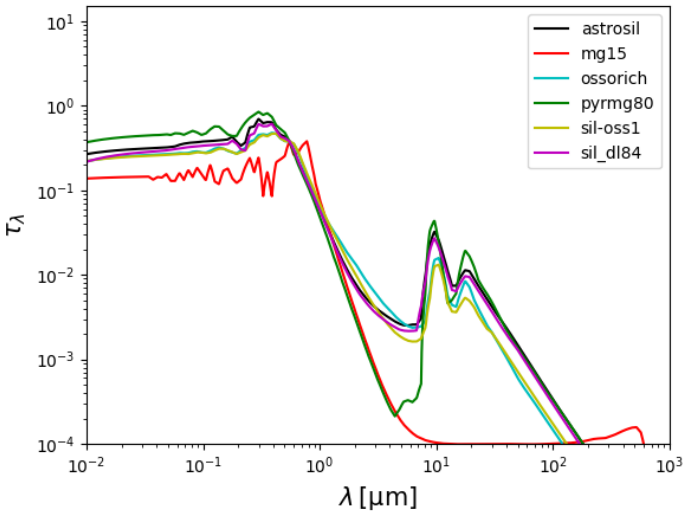

Figure 2.1: Optical depth of each silicate material studied by wavelength calculated with single grain sized models of $a = 0.15\,\mu$m, $R_{\rm int} = 10\,R_\star$ and $\tau_{\rm V} = 10$. *mg15*, Mg(1.5) SiO(3.5), corresponds to a magnesium silicate from Jäger et al. (2003). *pyrmg80*, Mg(0.8) Fe(0.2) SiO(3), corresponds to a magnesium-iron silicate from Dorschner et al. (1995). *astrosil* corresponds to an astronomical silicate from Laor and Draine (1993). *sil_ dl84* corresponds to an astronomical silicate from Draine and Lee (1984a). *ossorich* and *sil-oss1* are, respectively, the oxygen rich interstellar silicate and the astronomical silicate grains of Ossenkopf et al. (1992).

literature, this is commonly described by a probability density function of the type

$$f(a) = C(q)\ a^{-q}, a_{min} < a < a_{max}\,, \tag{2.2}$$

where C is a normalization constant and q is the power-law exponent. The larger q, the larger the fraction of small grains in the mixture. a_{min} and a_{max} correspond to the lower and upper limits of the distribution, respectively. Such function was first proposed in the pioneering work of Mathis et al. (1977) that used the above expression to model the interstellar extinction law. They found q to be quite uniform around the value of 3.5 for many different lines of sight, indicating a common process for the formation of dust grains in the interstellar medium. Until now, more than 3000 articles have applied this distribution on their works, some of the most remarkable ones are Draine and Lee (1984b), Savage and Mathis (1979) and Wilms et al. (2000).

The origin of the dust in the interstellar medium is a question still open for debate,

however red giant and supergiant stars are considered to be one of the sources of the interstellar dust (Levesque 2017). Dust grains are expected to form in their dense and cold outflows, and subsequently expelled by the stars, enriching the insterstellar medium. Providing that the nature of the dust in the interstellar medium does not change too strongly with time, one could expect that the dust grains in RSG outflows would bear similarities with the interstellar dust. With that in mind, modelling the circumstellar dust by the same type of distribution (Eq. 2.2) of the interstellar dust may provide us insights on the origin of the interstellar dust.

2.4 Building a grid of models for VY CMa

In order to model the SED of VY CMa (Fig. 1.2) using both HDUST and MCMC (see bellow), a grid of models is necessary that explores all the relevant range of model parameters. Before building the grid, however, it was necessary to understand and quantify the correlation between the most natural parameters of the problem ($\tau_{\rm rep}$ and $T_{\rm int}$) and the input parameters and values of HDUST ($\tau_{\rm V}$ and $R_{\rm int}$), where $\tau_{\rm V}$ stands for the optical depth at $V = 0.55\,\mu$m and $R_{\rm int}$ for the internal radius of the envelope. The solution obtained was to create a routine that could automatically run a small grid of 20 models (5 values of $R_{\rm int}$ and 4 of $\tau_{\rm V}$) for each distribution of grain size and calculate the $\tau_{\rm rep}$ and $T_{\rm int}$ of each model. With the correlation of ($R_{\rm int}$, $\tau_{\rm V}$) to ($\tau_{\rm rep}$, $T_{\rm int}$) for the 20 models, the routine interpolated in logarithmic scale to find the best pair of ($R_{\rm int}$, $\tau_{\rm V}$) for the adopted values for the grid of ($\tau_{\rm rep}$ and $T_{\rm int}$). In the case that a grid value is outside the 20 models range, the routine extrapolated via linear regression in logarithmic scale.

The reprocessing optical depth $\tau_{\rm rep}$ can be easily estimated from a HDUST simulation as follows. HDUST keeps track of the origin of the photons that escape the envelope. This origin can be either stellar emission or envelope emission. By integrating the total envelope emitted flux from the model, we obtain $L_{\rm rep}$ of Eq. 1.1. This can be seen in Figure 2.2, which shows an example model with $a_{\rm min} = 0.001\,\mu$m, $a_{\rm max} = 400\,\mu$m, $q = 2.5$, $R_{\rm int} = 20.86\,R_\star$ and $\tau_{\rm V} = 3.61$. The black line shows the emergent SED (stellar and dust contributions), the blue one the emitted spectrum from the envelope, the green line the transmitted spectrum (i.e., stellar light that did not interact in any way with the envelope) and the red line, the scattered flux. Applying the procedure above resulted in $\tau_{\rm rep} = 2$,

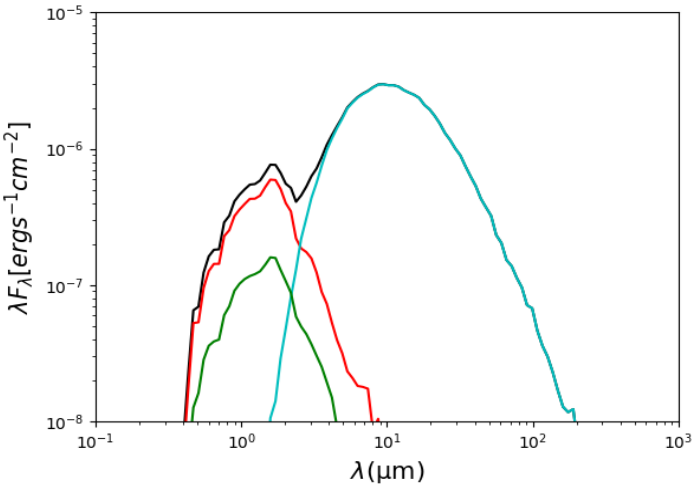

Figure 2.2: Example SED tracking the origin of each component of the total emergent flux. The black curve represents the emergent flux, the blue curve represents the envelope emitted flux (i.e. reprocessed photons), the red curve represent the scattered flux (i.e. photons that got scattered but not absorbed) and the green curve represents the transmitted flux (i.e. photons that did not interact with the dust). The parameters of the model are $a_{\rm min} = 0.001\mu$m, $a_{\rm min} = 400\mu$m, $q = 2.5$, $R_{\rm int} = 20.86R_\star$ and $\tau_{\rm V} = 3.61$.

meaning that that 86.5% of all photons came from the envelope.

With the relations between ($\tau_{\rm rep}$ and $T_{\rm int}$) to ($\tau_{\rm V}$ and $R_{\rm int}$) at hand, we computed the grid presented in Table 2.2, resulting in 5880 models. Each model was calculated by the HDUST code, which is in charge of performing the radiative transfer considering each variable as input. HDUST provides, as output, the emergent SED as well as the temperature structure of the grains.

After the grid was built and computed, the EMCEE code (Foreman-Mackey et al. 2013), which is a Python language implementation of the Bayesian inference and Monte

Table 2.2 - Grid values for the dust parameters around VY CMa.

$\tau_{\rm rep}$	$T_{\rm int}$[K]	$a_{\rm min}[\mu$m]	$a_{\rm max}[\mu$m]	q
1.0	900	0.001	1	2.5
1.5	1000	0.01	4	3.0
2.0	1100	0.1	10	3.5
2.5	1200	1	40	4.0
3.0	1300		100	4.5
3.5	1400		400	
4.0	1500			

Carlo Markov Chain method, was used to calculate the posterior distribution (P(H|E)) of each parameter using the Bayes theorem,

$$P(H|E) = \frac{P(E|H) \times P(H)}{P(E)}\,, \tag{2.3}$$

where $P(H)$ is the prior that encompasses any previous information available, $P(E|H)$ is the likelihood (which is related to an adopted merit function), and $P(E)$ is a normalization factor. P(H|E) is known as the posterior probability (or posterior, for short), which encompasses the information updated by an event, in our case, each event is the comparison between a combination of parameters and the observed SED. In EMCEE, the posterior is calculated from a distribution of walkers and steps, each walker being a mathematical sample whose initial position is randomly chosen and each subsequent step is decided based on a merit function (in our case, the inverse of the χ^2 [3] is used, implying that the greater the difference between the data and the model, the less likely it is for the model to represent the data). After all walkers have completed their own path, the resulting posterior probabilities of each model parameters can either be plotted in the so-called corner plots (an example is given in Fig. 3.2) or can be used to estimate the parameter value within a given range, reflecting a choice for the confidence level of the estimate. In all subsequent values and plots, we chose a confidence interval of 68 %.

[3] We adopted a variation of χ^2 that considers a distribution in a logarithmic scale, as in astronomy the events are commonly logarithmically distributed. $\chi^2 = (\log(F_{\rm obs}) - \log(F_{\rm mod}))/\sigma$, where $F_{\rm obs}$ is the observed flux, $F_{\rm mod}$ is the flux of each model and σ is the uncertainties in $F_{\rm obs}$.

Chapter 3

Modelling the circumstellar dust

We employed a Bayesian statistical analysis of the problem to unveil how much information about the grain sizes are imprinted on the SED. To achieve this, we computed a large grid of models for VY CMa, using the best parameters about the central star available in the literature, and explored different grain sizes distributions, ranging from very small to very large grains. The fitted parameters were the reprocessing optical depth ,$\tau_{\rm rep}$, the internal temperature, $T_{\rm int}$, smallest grain size, $a_{\rm min}$, largest grain size, $a_{\rm max}$, and the exponent of the power-law, q. The $a_{\rm min}$, $a_{\rm max}$ and q represent the distribution of Eq. 2.2.

In addition to the physical parameters above, all intrinsic to the system, we also fit the interstellar extinction, $E(B-V)$, ranging from 0 – 3, an interval range from the lowest expected value $E(B-V)=0$, to an upper interval greatest than the highest value found in the literature. Shenoy et al. (2016) estimated the interstellar extinction ($A_{\rm V}$) to an upper limit of 1.5, which corresponds to $E(B-V)=0.48$, for $R_{\rm V}=\frac{A_{\rm V}}{E(B-V)}=3.1$.

3.1 Most probable values for the model parameters

The results of a long MCMC simulation for VY CMa are shown in Figures 3.1 and 3.2. We used 300 walkers and 2000 steps. The first 1000 steps were removed from the chains for calculating the final probability density functions (PDFs) of each parameter. As EMCEE does not have a good behavior when the observed data has too many data points in a given wavelength region, as such region would dominate the χ^2 value, we adopted the option of binning the observed SED seen in Figure 1.2, so that the data points of the SED is equally distributed in logarithmic scale.

The blue curve of Figure 3.1 represents a model computed with the most probable

Table 3.1 - Best values for the dust parameters around VY CMa.

$a_{\rm min}[\mu{\rm m}]$	$a_{\rm max}[\mu{\rm m}]$	q	$\tau_{\rm rep}$	$T_{\rm int}[K]$	$E(B-V)$
0.002 ± 0.001	158^{+23}_{-3}	$3.47^{+0.03}_{-0.01}$	2.51 ± 0.01	1075^{+2}_{-11}	$0.22^{+0.01}_{-0.04}$

values of each parameters, which are given in Table 3.1. The model reproduces the data remarkably well, with the vast majority of the points less than 3-σ away from the observations. An exception for this is seen on the UV part of the spectrum, where the data presents a large scatter not reproduced by the models.

For all parameters, the resulting PDFs have a clear main peak, even though some have a secondary peak (Fig. 3.2), indicating a strong probability around a narrow value range (in other terms, good convergence was achieved).

Figure 3.3 shows, in a more quantitative way, how the parameters correlate or anti-correlate with each other. In this Figure, the two-by-two correlations are calculated by the Pearson correlation method (Hollander et al. 2013), according to which, the correlation ($C_{\rm X,Y}$) between two parameters, X and Y, is defined as

$$\mathrm{C_{X,Y}} = \frac{\mathrm{cov(X,Y)}}{\sigma_{\rm X}\sigma_{\rm Y}}\,, \tag{3.1}$$

where cov(X, Y) is the covariance between X and Y, and $\sigma_{\rm X}$, $\sigma_{\rm Y}$ are the standard deviations of each parameter. The correlations will be further discussed in Sect. 3.2.

3.2 Understanding the effect of each parameter

To better understand the effect of each parameter on the SED, and to perform an independent verification of the results shown in Figures 3.1 and 3.2, in this section we explore how varying each parameter, while keeping the others fixed at their values of Table 3.1, alters the model results.

3.2.1 Effects of the reprocessing optical depth

The parameter $\tau_{\rm rep}$, which is related to the amount of dust present, is the one that affects most the SED. Figure 3.4-a reveals that higher $\tau_{\rm rep}$ means more absorption in the UV region and more emission in the IR region. This is very straightforward to understand because of the definition of $\tau_{\rm rep}$ (Eq. 1.1): growing values of $\tau_{\rm rep}$ increase the fraction of

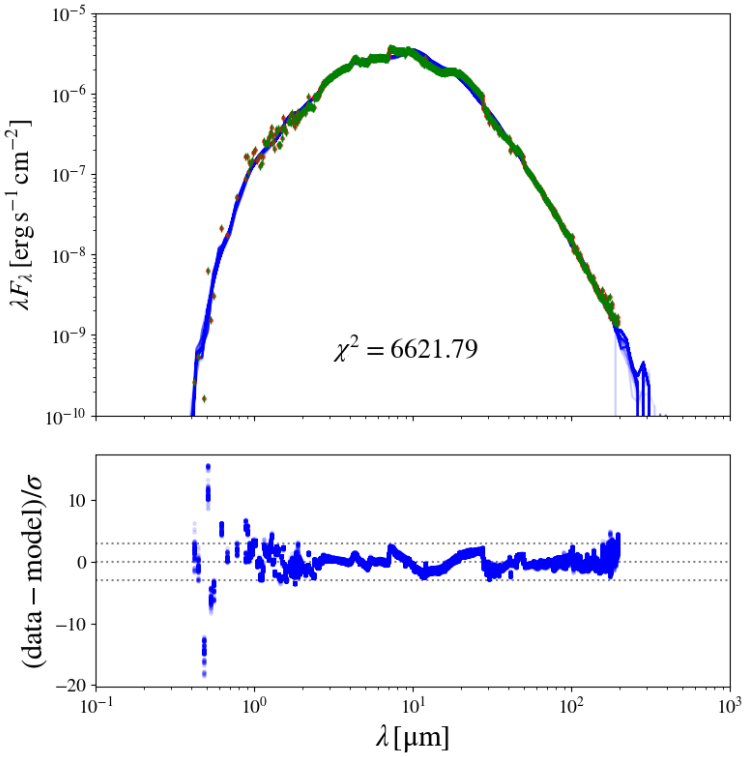

Figure 3.1: Model results for VY CMa. Top: comparison of the binned SED (green points) with the most-probable model (blue curves) computed with the values of Table 3.1. The χ^2 of this model is also indicated. Bottom: model residuals normalized by the observation uncertainties. The horizontal line indicate a 3-σ deviation from the model.

star light that is reprocessed into the IR domain, thus causing a corresponding decrease of the flux values at shorter wavelengths. It is important to note that extreme values of $\tau_{\rm rep}$ adopted in our grid clearly do not represent well the observations, indicating that the grid values were chosen properly.

3.2.2 Effects of the internal dust temperature

The internal temperature of the dust ($T_{\rm int}$), which is related to the internal radius of the envelope, affects mainly the peak wavelength of the dust emission, as per the well-known Wien's displacement law. In Figure 3.4-b, the shifting of the peak emission to longer wavelengths as the temperature decreases is visible. It is important to note that the dust temperature (around $1000K$) is much smaller than the stellar temperature (around $3490K$).

Fig. 3.3 shows that $T_{\rm int}$ strongly correlates with $E(B-V)$, which is expected since larger values of $T_{\rm int}$ would increase the short wavelength flux, requiring larger values of $E(B-V)$ to compensate from it. $T_{\rm int}$ anti-correlates strongly with q, which will be discussed below.

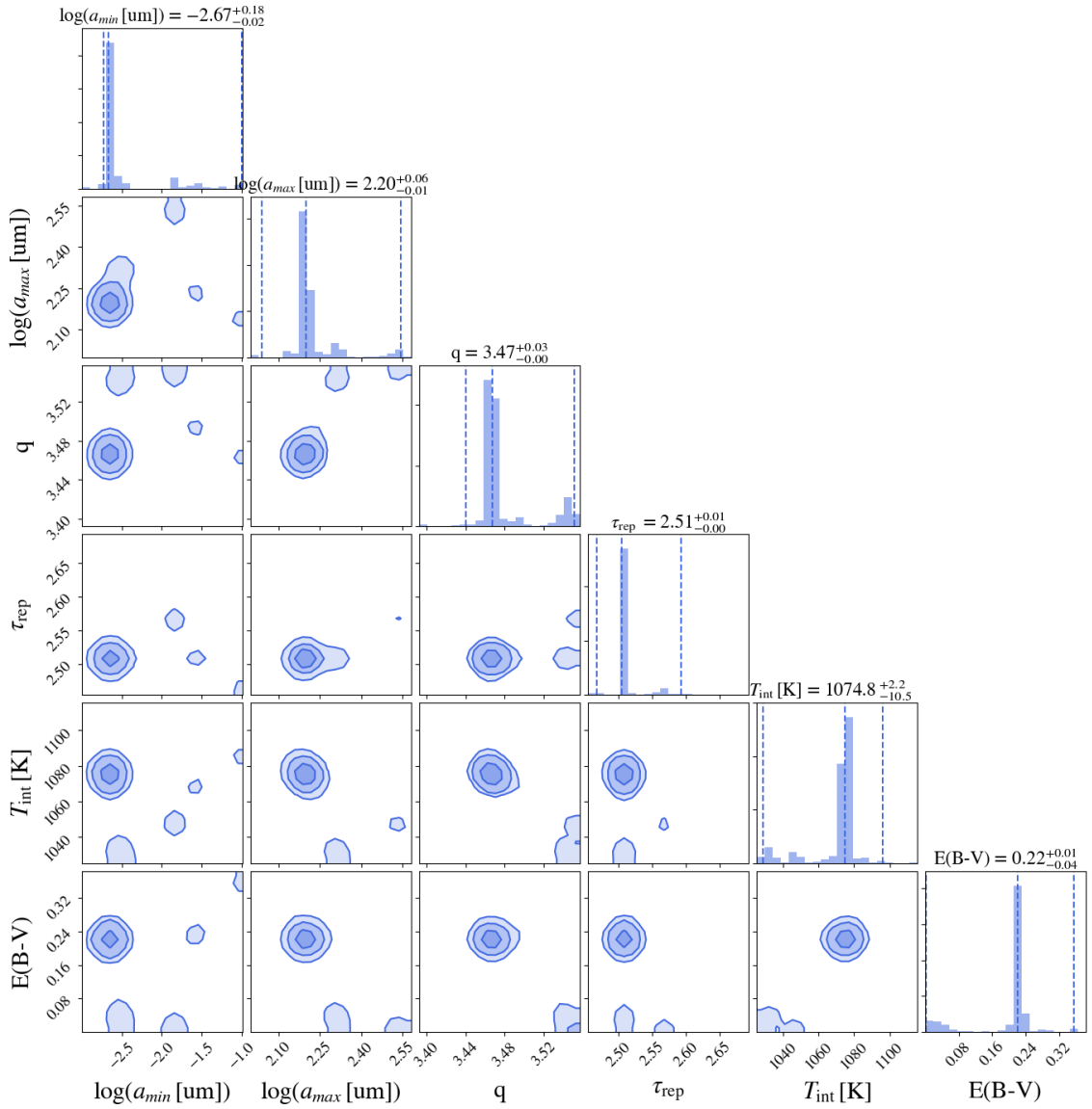

Figure 3.2: Corner plot representation of the output parameters of the MCMC run. The main diagonal plots show the PDFs of each parameters, with a parameter range estimate with 68% confidence level printed on top. The off-diagonal plots indicate the two-by-two correlations of each parameter.

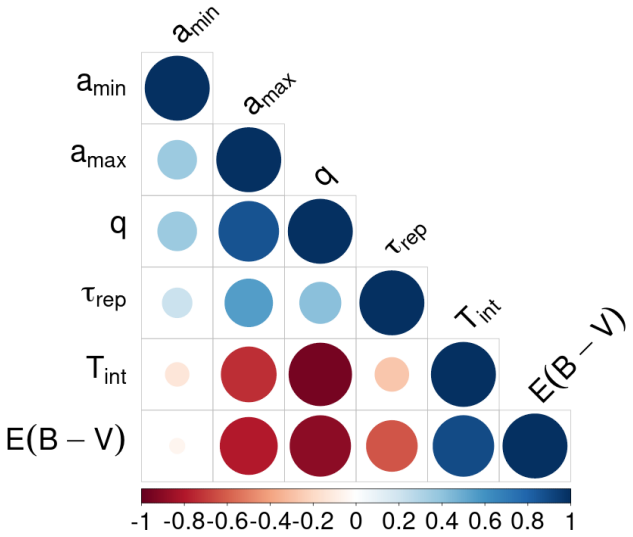

Figure 3.3: Correlation plot for EMCEE output. Each square correspond to the value of the two-by-two correlation, computed by applying the Pearson correlation method to the final chains of the MCMC run. The bluer the square, the more correlated are the parameters, the redder, the more anti-correlated.

3.2.3 *Effects of the interstellar extinction*

The interstellar extinction $E(B-V)$ is a well-known parameter whose effect is most important for shorter wavelengths. Indeed, Fig. 3.4-c shows exactly this behavior, with the model with low $E(B-V)$ (red) displaying much larger flux values at the UV, visible and near IR than the model with high $E(B-V)$. As it happened with the other parameters studied so far, the range chosen for $E(B-V)$ in our grid (Tab. 3.1) seems to have been properly chosen.

3.2.4 *Effects of grain size*

The dust grain size (a) has a more complex impact on the SED. In Figure 3.5, we see the effects that different grain sizes have on the pattern of the dust optical depth and how this changes the SED. Shown are simple models with a single grain size ($a = 0.005\,\mu$m and $a = 100\,\mu$m) for which the values of $T_{\rm int}$, $\tau_{\rm rep}$ and $E(B-V)$ were chosen to best approximate the single grain size models to the observed SED. The model with smaller

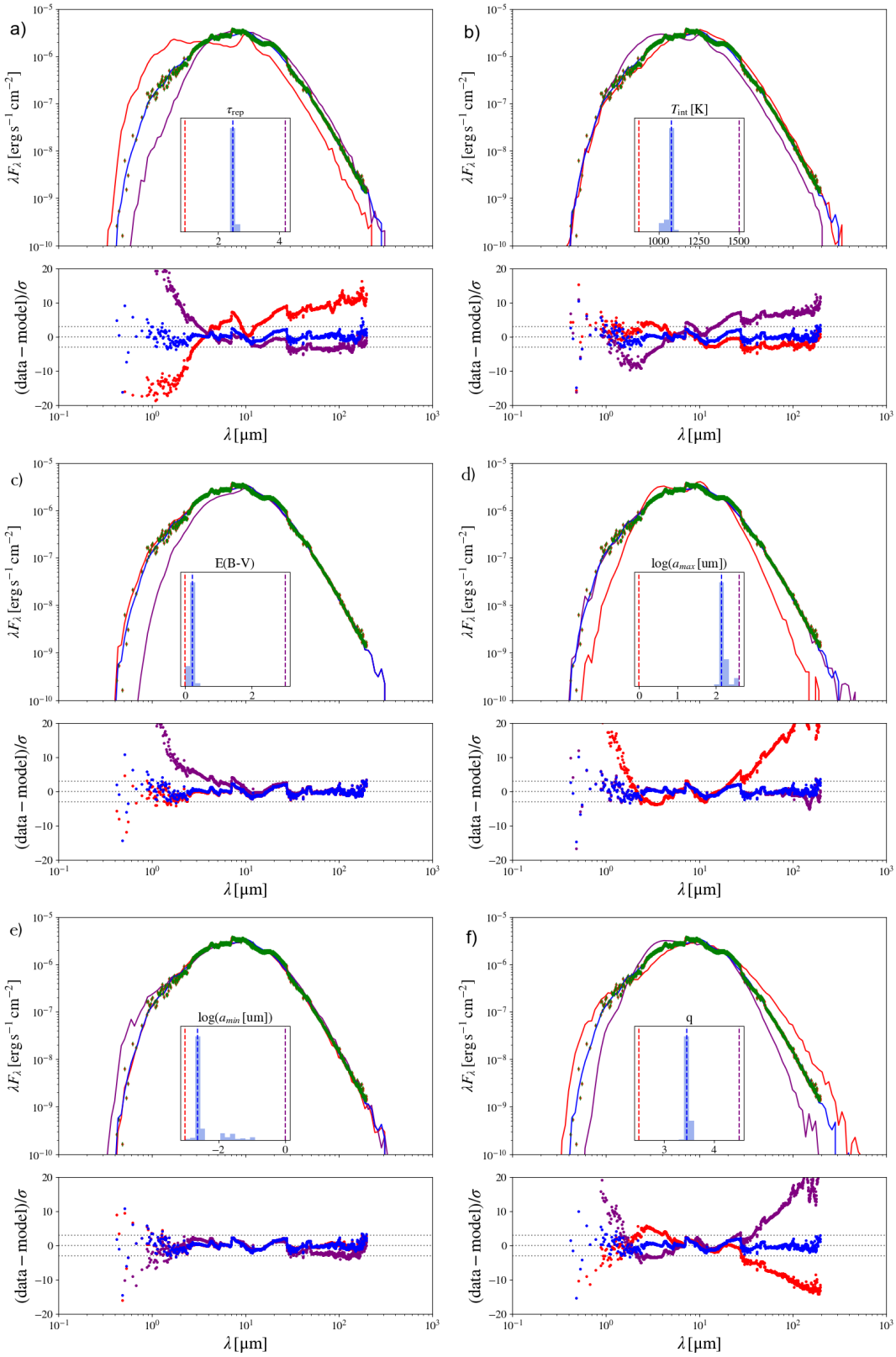

Figure 3.4: Effects of each parameter (a - $\tau_{\rm rep}$, b - $T_{\rm int}$, c - $E(B-V)$, d - $a_{\rm max}$, e - $a_{\rm min}$ and f - q) on the model SED. The model in blue is the same model shown in Fig. 3.1. The models in red and purple represent the extreme values of each parameter in our grid.

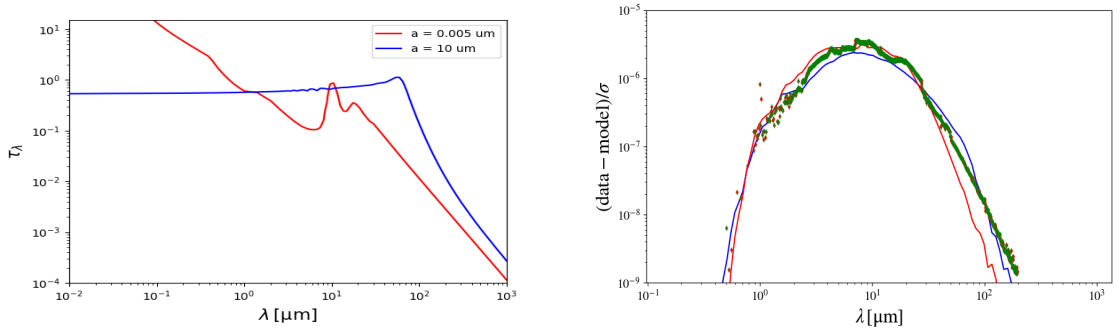

Figure 3.5: The effect of grain size, a, on the radial optical depth (left) and emergent flux (right). Shown are single-grain sized models, whose parameters are further described in the text.

grains correspond to $T_{\rm int} = 890\,{\rm K}$ and $E(B-V) = 0$, the other to $T_{\rm int} = 1100\,{\rm K}$ and $E(B-V) = 1.17$. Both models have the same $\tau_{\rm rep} = 1.86$. To better understand the optical depth pattern, let us study three different wavelength regimes. When the dust grain is much smaller than the wavelength, the opacity is in the so-called Rayleigh regime, which dictates that the amount of absorption is inversely proportional to the inverse of the wavelength, while the amount of scattering is proportional to the fourth power of the wavelength. When the opposite occurs, in the geometrical limit, the dust acts like a solid obstacle, which explains why that, for low wavelengths, the absorption coefficient is basically constant. In the intermediate regime, grain size comparable to wavelength, the opacity is given by the complex interaction of light with the dust refractory material, according to the Mie theory (Carciofi 2001, and references therein).

It is possible to notice in Figure 3.5 that neither grain size can successfully fit the whole SED, however each one represents better some part of it. The larger grains are better at fitting the long wavelengths ($\lambda > 40\,\mu$m) and the smaller grains fit better the mid SED ($2\,\mu{\rm m} < \lambda < 40\,\mu{\rm m}$). This demonstrates that a grain size distribution is needed in order to represent the observed SED, as seen in Fig 3.1. [1]

The value of the largest grain in the distribution, $a_{\rm max}$, as seen in Figure 3.4-d, has a strong impact in the very long wavelengths, which is due to the fact that large grain sizes have a larger opacity at large wavelength (Fig. 3.5), with a correspondingly larger emission,

[1] Even the larger grains could not perfectly fit the long wavelengths. In the *Trabalho de Graduação I*, we reported several attempts to fit the entire SED with a single grain sized model. Two possibilities considered were changing the density slope of the dusty shell (Eq. 2.1) and changing the dust composition. However none possibility could successfully fix the different slope in long wavelengths without producing any other features in the SED.

as per the well-known Kirchhoff law. This analysis suggest the existence of very large dust grains, 200 μm, surrounding VY CMa. Figure 3.3 shows that $a_{\max}$ is anti-correlated with $T_{\rm int}$. This happens because, as seen in Fig. 3.4-d, increasing $a_{\max}$ has a somewhat similar effect than decreasing $T_{\rm int}$.

The size of the smallest grains, $a_{\min}$, affects the SED in a very different way, basically increasing flux attenuation at short wavelengths as decreasing values are considered. However, we see, in Figure 3.4-e, that models with $a_{\min} \lesssim 0.2\mu$m are all very similar, indicating that this parameter is poorly constrained by the observations. This is reflected on the formal uncertainties derived for it in the previous section, which have larger upper limit errors. However, we believe that the PDF for $a_{\min}$ shown in Fig. 3.2 should not be taken blindly, as varying $a_{\min}$ in the range 0.001 — 0.2 μm have a very minimal effect on the SED. What can be said with some degree of confidence about $a_{\min}$ is that it should be smaller than about 0.2 μm.

3.2.5 Power-law exponent and its relation with the interstellar dust

The exponent of power-law, q, changes the relative fraction of small and large grains in the distribution. As seen in Figure 3.4-f, higher values of q means fewer large grains (resulting in lack of flux in long wavelengths) and more small grains (resulting in lack of flux in UV/visible and strong flux in the near/mid infrared). As q has a quite strong effect both on the short and long wavelength extremes of the SED, it also displays strong correlations or anti-correlations with parameters that also affect one of these regions (see. Fig. 3.3).

The best value of $q = 3.47^{+0.03}_{-0.01}$ is especially very interesting. As explained in Section 2.3, Mathis et al. (1977) found $q \approx 3.5$ for the interstellar medium, and the fact that our results for VY CMa matches this result is remarkable, as it may provide evidence that some of the interstellar dust grains are indeed formed in the strong outflows of evolved stars. Furthermore, this result may also indicate that the grain size distribution in the interstellar medium does not change much over time. A study comparing the value of q for several other supergiant stars could shed a light in the contribution of RSGs to the interstellar medium or even in mass loss and dust formation.

Chapter 4

Summary of developed work and future perspectives

This work has successfully characterized the dust around VY CMa, using a new approach with the MCMC and Bayesian inference background. A remarkable fit of the entire SED was achieved with the parameters shown in Table 3.1. In particular, the model was able to reproduce correctly the slope and level of the SED in the far infrared. This was only achieved after adopting a grain sized distribution. Recall that none of the models shown in the *Trabalho de Graduação I*, which were composed of single grain sizes, could reproduce this part of the SED satisfactorily.

The value of q shows a very interesting similarity to the value obtained by Mathis et al. (1977) in their study of the interstellar medium composition. This indicates a connection between the grains around RSGs, such as VY CMa, and the grains in the interstellar medium, contributing to the hypothesis that RSGs contribute to the dust enrichment of the interstellar medium. The obtained value for $E(B-V)$ is lower than the literature value. Shenoy et al. (2016) estimated the interstellar reddening (A_{V}) to an upper limit of 1.5 (which corresponds to $E(B-V) = 0.48$, for $R_{\mathrm{V}} = 3.1$). However their modelled SED clearly lacks flux in shorter wavelengths, which might affect negatively their ability to estimate properly the interstellar reddening. Therefore, $E(B-V) = 0.22$ seems to be realistic.

We are writing an article, which will be submitted in a few months, detailing this work. One of the next steps planned for the article is a deeper study on a_{min}, since this parameter was, it seems, too well constrained by EMCEE, with a precision much larger than what can be expected from a visual inspection of the models. Next, we plan to use mass loss rate estimates for VY CMa in the literature to estimate the mass density of the dust grains. Our results above provide a solid estimate of the number density of grains, but in order to

estimate the mass density we need to know the bulk density of the grain material. Also, the student will apply to a direct PhD program at IAG/USP and he intends to continue using this approach to study other RSGs in a future collaboration with an IC student, Lucas Paulino Santos. The main idea is to increase the sample of RSGs studied by our novel approach.

Bibliography

Carciofi A., PhD Thesis, 2001

Carciofi A. C., Bjorkman J. E., The Astrophysical Journal, 2006, vol. 639, p. 1081

Carciofi A. C., Bjorkman J. E., The Astrophysical Journal, 2008, vol. 684, p. 1374

Carciofi A. C., Bjorkman J. E., Magalhaes A., The Astrophysical Journal, 2004, vol. 604, p. 238

Danchi W., Bester M., Degiacomi C. G., Greenhill L., Townes C., The Astronomical Journal, 1994, vol. 107, p. 1469

Dorschner J., Begemann B., Henning T., Jaeger C., Mutschke H., A&A, 1995, vol. 300, p. 503

Draine B. T., Lee H. M., ApJ, 1984a, vol. 285, p. 89

Draine B. T., Lee H. M., ApJ, 1984b, vol. 285, p. 89

Foreman-Mackey D., Hogg D. W., Lang D., Goodman J., Publications of the Astronomical Society of the Pacific, 2013, vol. 125, p. 306

Hollander M., Wolfe D. A., Chicken E., John Wiley & Sons, 2013

Humphreys R. M., Ziurys L., Bernal J., Gordon M. S., Helton L. A., Ishibashi K., Jones T. J., Richards A., Vlemmings W., The Astrophysical Journal Letters, 2019, vol. 874, p. L26

Ivezic Z., Nenkova M., Elitzur M., ascl, 1999, pp ascl–9911

Jäger C., Dorschner J., Mutschke H., Posch T., Henning T., A&A, 2003, vol. 408, p. 193

Joint Iras Science W. G., , 1994, vol. 2125

Kurucz R., Kurucz CD-ROM No. 19. Cambridge, Mass.: Smithsonian Astrophysical Observatory, 1994, vol. 19

Laor A., Draine B. T., ApJ, 1993, vol. 402, p. 441

Levesque E. M., IOP Publishing, 2017, pp 13–14,39–43

Mathis J. S., Rumpl W., Nordsieck K. H., The Astrophysical Journal, 1977, vol. 217, p. 425

Ossenkopf V., Henning T., Mathis J., Astronomy and Astrophysics, 1992, vol. 261, p. 567

Savage B. D., Mathis J. S., ARA&A, 1979, vol. 17, p. 73

Scalise Jr E., Lepine J., A&A, 1978, vol. 65, p. L7

Scicluna P., Siebenmorgen R., Wesson R., Blommaert J., Kasper M., Voshchinnikov N., Wolf S., Astronomy & Astrophysics, 2015, vol. 584, p. L10

Shanks T., Metcalfe N., Chehade B., Findlay J. R., Irwin M. J., Gonzalez-Solares E., Lewis J. R., Yoldas A. K., Mann R. G., Read M. A., Sutorius E. T. W., Voutsinas S., MNRAS, 2015, vol. 451, p. 4238

Shenoy D., Humphreys R. M., Jones T. J., Marengo M., Gehrz R. D., Helton L. A., Hoffmann W. F., Skemer A. J., Hinz P. M., The Astronomical Journal, 2016, vol. 151, p. 51

Stothers R. B., Chin C.-W., The Astrophysical Journal, 1996, vol. 468, p. 842

Wilms J., Allen A., McCray R., ApJ, 2000, vol. 542, p. 914

Wittkowski M., Hauschildt P., Arroyo-Torres B., Marcaide J., Astronomy & Astrophysics, 2012, vol. 540, p. 4